



TECHNISCHE
UNIVERSITÄT
WIEN
Vienna University of Technology



Massachusetts
Institute of
Technology

Final Report for Austrian Marshall Plan Foundation

Dynamic Stability Analysis of Nonlinear Systems

Subtitle

Dynamical behavior of moving load in interaction
with sheaves assembly in nonlinear systems

First Supervisor:

Prof. Dr. Georg Kartnig

M.Eng. Hesam Farhangfar

Institute of Engineering Design and Logistics

Faculty of Mechanical and Industrial Engineering

Technical University of Vienna

Massachusetts institute of Technology (MIT)

February 2018

Table of Contents

- 1 Introduction 2
 - 1.1 Statement of Problem 2
 - 1.2 Objectives and Research Methodology 2
 - 1.3 Research Structure 2
- 2 Simulation and analysis 5
 - 2.1 Defining the rope as a continuum 5
 - 2.2 Numerical vs analytical Solutions for rope system 5
 - 2.3 Mathematical background of the Galerkin method 6
 - 2.4 Sheaves simulation in three levels10
 - 2.4.1 Modeling the first level with fixed sheaves10
 - 2.4.2 Modeling the second level with vertically free sheaves15
 - 2.4.3 Modeling the third level with vertically and rotationally free sheaves19
 - 2.5 Contact Mechanics 25
- 3 Limits of the semi-analytical solution on moving load 27
- 4 Conclusion 29

1 Introduction

1.1 Statement of Problem

There are unwanted vibrations in ropeway systems that makes them unstable. This dissertation is a part of an ongoing project of Austrian Research Agency (FFG) in cooperation with Doppelmayr Group and will try to find solutions and concepts to optimize the vehicle dynamics and reduce the vibration of ropeway systems.

This dissertation will use the existing end results of the previous academic thesis to implement methods for reducing the vertical vibration of the system and will focus mainly on sheaves assembly.

1.2 Objectives and Research Methodology

The dissertation is based on top-down approach and first tries to convert the mechanical model to a simplified mathematical and physical model. Variety of optimization processes are used to find the solution. Some parts are solved exact and analytically and some part which cannot solved exactly are simplified and adapted to numerical and approximated solution.

In conclusion follows the improvement suggestions to make the real system stable.

1.3 Research Structure

The research consists of four main parts.

Simulations in three levels: The simulations are splatted in to three levels to have a better understanding of the system. In each level the complexity of the system increases and finally the last and third level represents the main and real physical system that is being researched.

Verifications of the simulation results: Validating the results of the simulation will be by means of the experimental results. For this reason, even after having the 3rd level of the simulation, we need a model that has the same system parameters as on the test facility and after adapting the last level of the simulation with the test facility the results (experimental, analytical and numerical) will be compared to find the acceptable variance and validating the system.

Theoretical analysis: After having a valid system, it is possible to work with the parameters that can influence the system. This part of expect on the test facility of real

system is not possible or very hard to consider. Therefore, a valid simulation will be a very good instrument that allows us to change the parameters and study the results. Also combining the system parameters is also possible to find the optimum point of the system and improve the dynamical stability of the system.

PI: Different levels of the simulations are defined to make the problem, objective and comprehensible. After simulating different levels, the final verification will occur between the theoretical and the measured data from the testing facility.

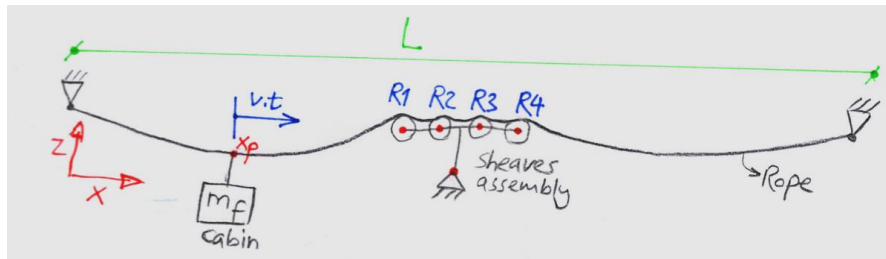


Figure 1 Free Body Diagram

PII: The simulations should be verified by means of the results of the test facility. This verification is necessary to find out if the system is simplified and simulated in the right way. The test facility includes the main parts of the system designed to measure the required parameters in different system condition.

The main focus in this dissertation will be on the sheaves assembly. The results of the other researches in this area is used to study the behavior of the sheaves in different system conditions to find the influence of different system parameters in interaction with sheaves assembly on the entire system.

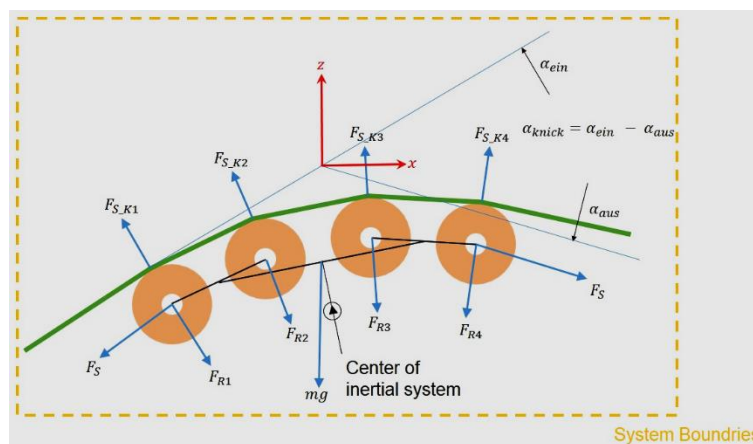
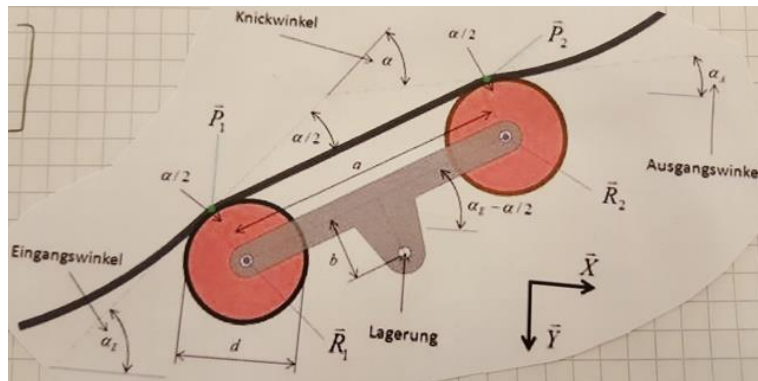


Figure 2 Free body 2

The system is reduced to two sheaves to make it comprehensible. This simplification will not influence the simulation results.



Reduced model from four sheaves to two sheaves in interaction with the rope

PIII: Theoretical analysis: Test facility has its own limits and boundaries that prevents studying some other physical phenomena that could occur in dynamical systems such as chaos and bifurcations. After verifying the simulation with the aid of measured data from the test facility, the system response is studied by considering the probability and influence of these physical phenomena.

PIV: After finalizing the theoretical in part one to three, a model reduction is needed to make the results of the study practical and operational for the real system. The results of this section is also used to optimize the system based on study results.

2 Simulation and analysis

2.1 Defining the rope as a continuum

Because of the complexity of the systems the simulations are based in three main levels beginning in the first level from two fixed sheaves which cannot vibrate, to the second level that includes the same sheaves which can just swing in the vertical direction and finally in the third level the system of sheaves assembly which are connected to each other and can swing in the both directions depending on the affecting forces. Matlab software is used to simulate this continuous system in all three levels.

Wave equation in general form is the basic module that helps to define the system:

$$\frac{\partial^2 u}{\partial t^2} = c^2 \nabla^2 u \quad (1.1)$$

C is a constant and ∇ is the Laplace operator. The adapted form of the wave equation which is used to define the rope which is also a partial differential equation of second order:

$$\mu \cdot \ddot{w} - s \cdot w'' = q(x, t) \quad (1.2)$$

In this equation the $q(x, t)$ is the inhomogeneous part of the time and position dependent equation which later will define each elements that is hanging on the rope.

2.2 Numerical vs analytical Solutions for rope system

A concentrated load acting on a continuous medium is usually described by a Dirac delta function. The point force or mass whose area of influence is limited, must be described in the entire spatial domain of the structure, for example $0 \leq x \leq l$. Multiplication of the force by the Dirac delta function (x) leads to such an effect. Then

we have the load terms $(x-x_0) P$ or $(x-x_0) m \frac{d^2 w}{dt^2}$ described in the domain of the problem. Unfortunately, the mathematical treatment of the term of the first type is

relatively simple. It does not contain the solution variable. The treatment of a term of the second type, which describes the inertial force induced by the material particle, is much more complex. It includes the acceleration of the selected point x_0 as the second derivative of the solution of the differential equation w . What is more, the argument $x_0 = vt$ moves with velocity v and the inertial term is a function of both x and t .

A semi analytical method is needed to solve the entire system of equations. In other words, the Galerkin method of weighted residual is used to solve the time-dependent part of the system numerically and Fourier series are used to solve the position-dependent part exactly, when it's solved for $n \rightarrow \infty$.

Due to the presence of the Dirac delta function in this result, the solutions obtained to these partial differential equations are not solutions in the classical sense, but are called 'weak' or 'distributional' solutions. So we must extend the concept of solution, arranging that any limit of an almost uniformly convergent sequence of classical

solutions will be regarded as a generalized solution in the sense of a distribution.

Distributions are therefore defined as the limit of sequences of continuous functions. This is called the sequential theory of distributions, in contrast to the functional theory. For each distribution in the sense of L. Schwartz (functional) there is exactly one distribution in the sense of Mikusiński–Sikorski (sequential), and vice versa, so there is a mutual uniqueness. Distributions are thus a generalization of functions. The purpose of the concept of a distribution is to give the correct meaning qua mathematical concept to objects such as the Dirac delta ($\delta(x)$), which is much used in mathematical physics. An important feature of a distribution is that it ensures the possibility of differentiation, which is not always allowed for an arbitrary set of functions. The starting point for the sequential theory of distributions is the set of functions which are continuous on some fixed interval $A < x < B$ ($\leq A < B \leq$). If a sequence $f_n(x)$ of such continuous functions converges almost uniformly to a function $f(x)$, it is also convergent in the sense of distributions to $f(x)$. Every convergent sequence of distributions can be differentiated term by term (analogous to a uniformly convergent series). Of course, every uniformly convergent sequence is convergent almost uniformly. This allows, in the distribution sense, the differentiation of any function, changing the order of differentiations, and passing to the limit, without any restrictions. Such a statement in classical analysis is in general not true and is only possible under additional assumptions.

2.3 Mathematical background of the Galerkin method

Galerkin method offers an approximate solution for the differential equations. The method of weighted residuals which is used here, helps to reformulate the equation by converting it from continuous to a discrete problem.

$$\begin{aligned} \mu \ddot{w} - (S W')' &= q(x,t) \quad \text{Starting point} \\ \tilde{w} &= \vec{c}^T(x) T(t) \quad \text{approximate solution} \\ e(x) &= \mu \ddot{\tilde{w}} - (S \tilde{w}')' - q(x,t) \quad \text{Residual} \\ \int_0^L e(x) y(x) dx &= 0, \quad y(x) = \vec{c}(x) \\ \int_0^L (\mu \vec{c}^T \ddot{\vec{c}} - (S \vec{c}^T T)' - q(x,t)) y &= 0 \\ \underbrace{\int_0^L \mu \vec{c} \vec{c}^T dx}_{M} \ddot{\vec{T}} - \underbrace{\int_0^L (S \vec{c}^T T)'}_{\text{partial integration}} \vec{c} dx - \int_0^L q(x,t) \vec{c} dx &= 0 \end{aligned}$$

If $q(x,t)$ considered as zero the system will be a simple homogenous wave equation. $q(x,t)$ will be the summary of all elements that we want to define inside the loop like sheaves, static and moving loads and other elements that have to be modelled mathematically. For each element, we will have one differential equation and finally the system of differential equations that are used as the input of the ODE solver in Matlab.

There also has to be considered that the method of partial integration is applied to solve the second term and the solution after reformulation there will be two terms that one of them will define the stiffness matrix and the other one will be the mass matrix.

$$\begin{aligned} \int_0^L \mu \vec{c} \vec{c}^T dx \ddot{\vec{T}} - \underbrace{\left[(S \vec{c}^T T) \vec{c} \right]_0^L}_0 - \underbrace{\int_0^L (S \vec{c}^T T)' \vec{c} dx}_K &= \\ \underbrace{\int_0^L q(x,t) \vec{c} dx}_E & \\ M = \int_0^L \mu \vec{c} \vec{c}^T dx \quad K = \int_0^L S \vec{c}' \vec{c}'^T dx, \quad E = \int_0^L q(x,t) \vec{c} dx & \\ \text{Final Formulation: } \boxed{M \ddot{\vec{T}} + K \vec{T} = E} & \end{aligned}$$

Both the mass and stiffness matrix are integral functions that has to be calculated separately in Matlab and the results will flow inside the numerical solver.

As seen the final formulation doesn't have the damping factor inside it because the system is internally and externally damped by means of the structure of the rope.

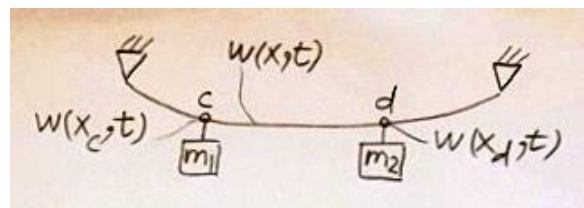
In most problems of mathematical physics, the true solutions are not smooth, i.e., they are not continuously differentiable. Thus, we cannot immediately apply a Galerkin approach. For example, in the equation of static mechanical equilibrium $\nabla \cdot \sigma + f = 0$, there is an implicit requirement that the stress, σ , is differentiable in the classical sense. Virtually the same mathematical structure form holds for other partial differential equations of mathematical physics describing diffusion, heat conduction, etc.

In many applications, differentiability is too strong a requirement. Therefore, when solving such problems we have two options: enforcement of jump conditions at every interface or; weak formulations (weakening the regularity requirements).

Weak forms, which are designed to accommodate irregular data and solutions, are usually preferred. Numerical techniques employing weak forms, such as the FEM, have been developed with the essential property that whenever a smooth classical solution exists, it is also a solution to the weak form problem. Therefore, we lose nothing by reformulating a problem in a more general way, by weakening the a priori smoothness requirements of the solution.

In the following few chapters, we shall initially consider a one-dimensional structure that occupies an open bounded domain in $\Omega \in \mathbb{R}$, with boundary $\partial\Omega$. The boundary consists of Γ_u on which the displacements (u), or any other primal variable (temperature in heat conduction applications, concentration in diffusion applications, etc. are prescribed and a part Γ_t on which tractions ($t = \sigma n$, n being the outward normal) are prescribed. We now focus on weak forms of a one-dimensional version of Equation.

Here is another formulation for the system of rope without sheaves assembly but with loads. The rope is fixed in both ends and there is a natural deflection that is comes from the weight of the rope. This system can still exactly calculated by means of differential equation. But if we want to make the system more complex by applying many loads or the accelerating or defining the sheaves assembly in exact points of the coordination this will lead to some integral functions that cannot be solved generally and exactly and has to be inserted to the numerical solver to find the answer area.



This is called a weak form because it does not require the differentiability of σ . In other words, the differentiability requirements have been weakened. It is clear that we are able to consider problems with quite irregular solutions. We observe that if we test the solution with all possible test functions of sufficient smoothness, then the weak solution is equivalent to the strong solution. We emphasize that provided the

true solution is smooth enough, the weak and strong forms are equivalent, which can be seen by the above constructive derivation.

$\mu \ddot{w} - S \dot{w}' = q(x,t) = -(F_{R1} + F_{R2}) f(x)$ $\ddot{w} - \frac{S}{\mu} \dot{w}' = -\frac{1}{\mu} (F_{R1} + F_{R2}) \cdot f(x) \text{ Dirac}$ $\ddot{w} - \omega_0^2 \dot{w}' = \frac{1}{\mu} (F_{R1} + F_{R2}) \cdot \vec{c}^T(x) A_n$ $F_{R1} = -K_R (y_1 - w(x_c, t))$ $F_{R1} = -K_R (y_1 - \vec{c}^T(x_c) \cdot T)$ $F_{R2} = -K_R (y_2 - \vec{c}^T(x_d) \cdot T)$ $m_1 \ddot{y}_1 = -m_1 g + F_{R1}$ $m_2 \ddot{y}_2 = -m_2 g + F_{R2}$ $\ddot{y}_1 = \frac{1}{m_1} F_{R1} - g$ $\ddot{y}_2 = \frac{1}{m_2} F_{R2} - g$ $w(x,t) = T(t) \vec{c}^T(x)$ $\dot{w}(x,t) = \dot{T}(t) \vec{c}^T(x)$ $\ddot{w}(x,t) = \ddot{T}(t) \vec{c}^T(x)$ $\dot{w}'(x,t) = -\left(\frac{n\pi}{L}\right)^2 \vec{c}^T(x) T(t)$	<p>* Ch.g.l. des Seils</p> $\ddot{T} \vec{c}^T + \left(\frac{\omega_0 n \pi}{L}\right)^2 T \vec{c}^T = \frac{1}{\mu} \cdot \vec{c}^T A_n \cdot K_R [y_1 + y_2 - (\vec{c}^T(x_c) + \vec{c}^T(x_d)) T]$ $\vec{c}^T \left[\ddot{T} + \left(\frac{\omega_0 n \pi}{L}\right)^2 T + \frac{1}{\mu} A_n K_R y_1 + \frac{1}{\mu} A_n K_R y_2 + \frac{1}{\mu} A_n K_R \vec{c}^T(x_c) T - \frac{1}{\mu} A_n K_R \vec{c}^T(x_d) T \right] = 0$ $I \ddot{T} = -\left[\left(\frac{\omega_0 n \pi}{L}\right)^2 + \frac{1}{\mu} A_n K_R \vec{c}^T(x_c) + \frac{1}{\mu} A_n K_R \vec{c}^T(x_d)\right] T + \frac{1}{\mu} A_n K_R y_1 + \frac{1}{\mu} A_n K_R y_2$ <p>* Ch.g.l. des Fahrzeuges</p> $II \ddot{y}_1 = -\frac{1}{m_1} K_R (y_1 - \vec{c}^T(x_c) T) - g = \frac{K_R}{m_1} \vec{c}^T(x_c) T - \frac{K_R}{m_1} y_1 - g$ $III \ddot{y}_2 = \frac{K_R}{m_2} \vec{c}^T(x_d) T - \frac{K_R}{m_2} y_2 - g$
--	---

Mathematically, a string is the simplest structure to be analysed. Engineering solutions frequently require the application of elements that resist tension but are flexible to bending, for example fibres, ropes, chains, or cables. Moreover, the same equation governs other physical problems such as the longitudinal vibrations of rods. First we will consider a massless string. The Fourier series are again used to define the points and the function of displacement for the both loads. There are also other numerical theorem as if Ritz method that can be used the find the numerical solution for the system.

2.4 Sheaves simulation in three levels

Previously defined system will be analyzed in a multi-level simulation method to have better understanding from the self-regulating sheaves in interaction with rope as a continuum. The complexity of the levels will increase in each step to finally have the real system that have vertical and rotational degrees of freedom.

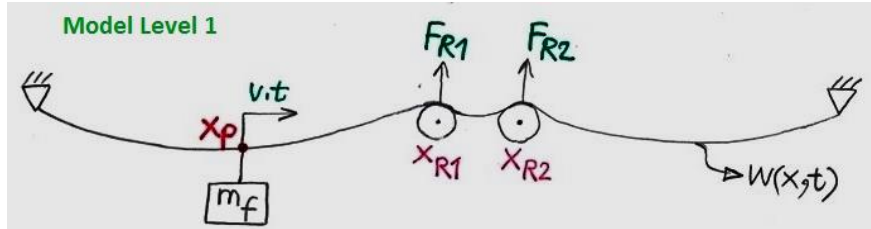
In each level the steady state of static results and dynamic results are presented and are compared to each other, also the feasibility of the results have been discussed.

The final results of the simulations in the third level will be adapted again to represent the test facility. The objective is to compare the simulated system to the real system to inspect if the system can be validated through the comparison and study the effects of different parameters on the system in the future.

2.4.1 Modeling the first level with fixed sheaves

In the first layer it's assumed that the sheaves are not connected to each other and are separately fixed on certain position of the rope.

The mass of the cabin m_f is also included to the rope.



$$\mu \cdot \ddot{w} - s \cdot w'' = \overbrace{-\mu \cdot g}^{\text{Gravity}} - \overbrace{F_{R1} \cdot f_1(x)}^{\text{First sheave}} - \overbrace{F_{R2} \cdot f_2(x)}^{\text{Second sheave}} - \overbrace{F_f \cdot f_f(x)}^{\text{Cabin}}$$

$$\mu \cdot \ddot{w} - s \cdot w'' = -\mu \cdot g - F_{R1} \cdot \delta(x - x_{R1}) - F_{R2} \cdot \delta(x - x_{R2}) - F_f \cdot \delta(x - x_p(t))$$

$$m_f \cdot \ddot{y} = -m_f \cdot g + F_f$$

$$F_{R1} = -k_R \overbrace{(w_{sp}(x_{R1}, t) - w(x_{R1}, t))}^{\text{Set point}}$$

$$F_{R2} = -k_R \overbrace{(w_{sp}(x_{R2}, t) - w(x_{R2}, t))}^{\text{Set point}}$$

Using the Galerkin method to solve the time dependent part numerically:

$$\overbrace{e(x)}^{\text{Residuum}} = \mu \cdot \ddot{w} - s \cdot w'' + \mu \cdot g + F_{R1} \cdot f_1(x) + F_{R2} \cdot f_2(x) - F_f \cdot f_f(x)$$

$$e(x) = \mu \cdot \ddot{w} - s \cdot w'' + \mu \cdot g + F_{R1} \cdot \delta(x - x_{R1}) + F_{R2} \cdot \delta(x - x_{R2}) - F_f \cdot \delta(x - x_p(t))$$

$$\int_0^L e(x) \cdot y(x) dx = 0 \quad , y(x) = \vec{C}(x)$$

$$M \cdot \ddot{T} + K \cdot T = +E_g - F_{R1} \cdot E_{R1} - F_{R2} \cdot E_{R2} - F_f \cdot E(t)$$

To calculate the static part, assumed that $M\ddot{T} = 0$ so the T will be:

$$T = K^{-1} \cdot E_g - K^{-1} \cdot F_{R1} \cdot E_{R1} - K^{-1} \cdot F_{R2} \cdot E_{R2} - K^{-1} \cdot F_f \cdot E(t)$$

And \ddot{T} for the dynamic side will be:

$$\ddot{T} = M^{-1} \cdot E_g - M^{-1} \cdot F_{R1} \cdot E_{R1} - M^{-1} \cdot F_{R2} \cdot E_{R2} - M^{-1} \cdot F_f \cdot E(t) - M^{-1} \cdot K \cdot T$$

Calculations for simulating the first level.

Diagram labels: grav, sheave 1, sheave 2, cabin, x_p , x_{R1} , x_{R2} , F_{R1} , F_{R2} , F_f , $v \cdot t$, $W(x,t)$.

$$\mu \ddot{w} - (S w')' = -\mu g - F_{R1} f(x_{R1}) - F_{R2} f(x_{R2}) - F_c f(x_p), \quad F_c = -m_f \cdot g$$

$$\mu \ddot{w} - (S w')' = -\mu g - F_{R1} \delta(x - x_{R1}) - F_{R2} \delta(x - x_{R2}) - F_f \delta(x - x_p(t))$$

$$m_f \ddot{y}_f = -m_f g + F_f \Rightarrow \ddot{y}_f = -g + \frac{F_f}{m_f}, \quad w(x,t) = T(t) \cdot \vec{C}(x)$$

$$F_f = -K_R (y_f - w(x_p(t), t)) = -K_R (y_f - \vec{C}(x_p(t)) \cdot T), \quad \vec{C}(x_p(t)) = \sin\left(\frac{\pi x_p}{L} \cdot v \cdot t\right)$$

$$F_{R1} = -K_R (w_{\text{soil}}(x_{R1}, t) - w(x_{R1}, t)) = -K_R (y_{R1} - \vec{C}(x_{R1}) \cdot T), \quad \vec{C}(x_{R1}) = \sin\left(\frac{\pi x_{R1}}{L}\right)$$

$$F_{R2} = -K_R (w_{\text{soil}}(x_{R2}, t) - w(x_{R2}, t)) = -K_R (y_{R2} - \vec{C}(x_{R2}) \cdot T), \quad \vec{C}(x_{R2}) = \sin\left(\frac{\pi x_{R2}}{L}\right)$$

$$e(x) = \mu \ddot{w} - (S w')' + \mu g + F_{R1} \delta(x - x_{R1}) + F_{R2} \delta(x - x_{R2}) + F_f \delta(x - x_p(t))$$

After applying Galerkin method to the fix sheaves in the first level of simulation, we will have:

$$e(x) = \mu \ddot{w} - (S\dot{w})' + Mg + F_{R1} \delta(x-x_{R1}) + F_{R2} \delta(x-x_{R2}) + F_f \delta(x-x_p(t))$$

$$\int_0^L e(x) y(x) dx = 0 \rightarrow y(x) = \vec{c}(x) \quad \text{Galerkin}$$

$$M\ddot{T} + KT = +Eg - F_{R1} E_{R1} - F_{R2} E_{R2} - F_f E(t)$$

Static: $M\ddot{T} = 0 \rightarrow T = K^{-1} Eg - K^{-1} F_{R1} E_{R1} - K^{-1} F_{R2} E_{R2} - K^{-1} F_f E(t)$

Dynamic $\rightarrow \ddot{T} = M^{-1} Eg - M^{-1} F_{R1} E_{R1} - M^{-1} F_{R2} E_{R2} - M^{-1} F_f E(t) - M^{-1} KT$

$$E_{R1} = \int_0^L f(x_{R1}) \vec{c}(x) dx = \int_0^L \delta(x-x_{R1}) \vec{c}(x) dx = \vec{c}(x_{R1}), E_{R2} = \vec{c}(x_{R2})$$

For code: static:

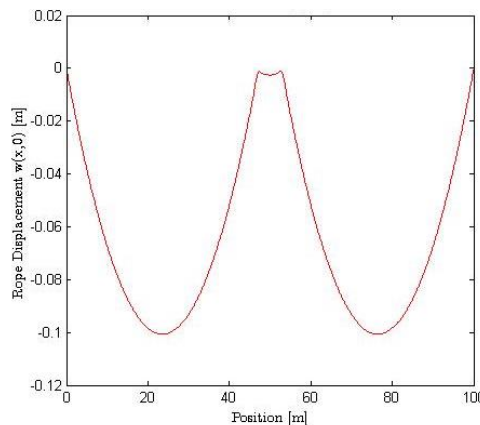
$$KT = Eg - (-K_R (y_{R1} - \vec{c}^T(x_{R1}) T)) E_{R1} - (-K_R (y_{R2} - \vec{c}^T(x_{R2}) T)) E_{R2} - (-K_R (y_f - \vec{c}^T(x_f))) E(t)$$

$$T = \text{inv}[K + K_R \vec{c}^T(x_{R1}) E_{R1} + K_R \vec{c}^T(x_{R2}) E_{R2} + K_R \vec{c}^T(x_f) E(t)] x_{\Delta}$$

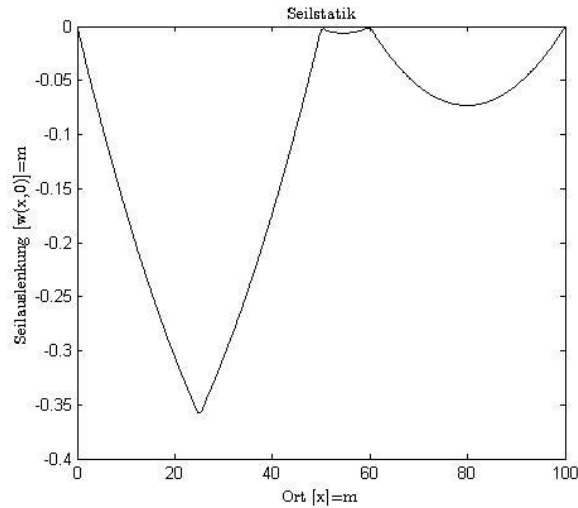
$$Eg - K_R y_{R1} E_{R1} - K_R y_{R2} E_{R2} - K_R y_f E_t \quad E(t) = -m_f \cdot g \cdot \sin\left(\frac{n\pi}{L} v \cdot t\right)$$

The simulation results below shows the fixed sheaves and the rope which is fixed on two points. The distribution is symmetrical because the mass is not included.

2.4.1.1 Static Simulation Results and discuss

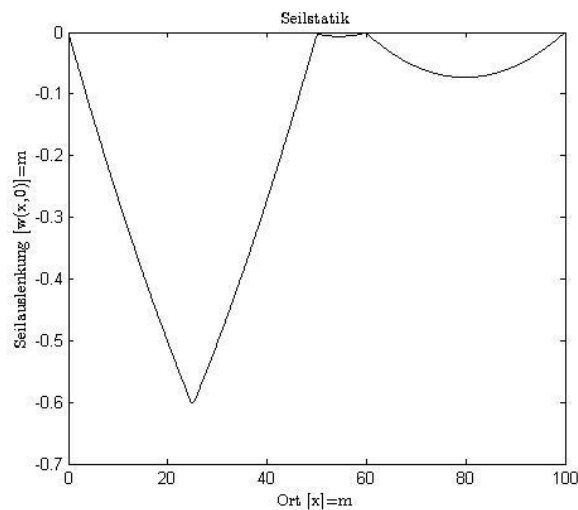


The other results shows the static results with the mass. The mass of the cabin m_f is 400Kg and it is positioned at 25m, the length of the rope is 100m and the fixed sheaves are positioned at 50m and 60m. (Gross et al. 2014)



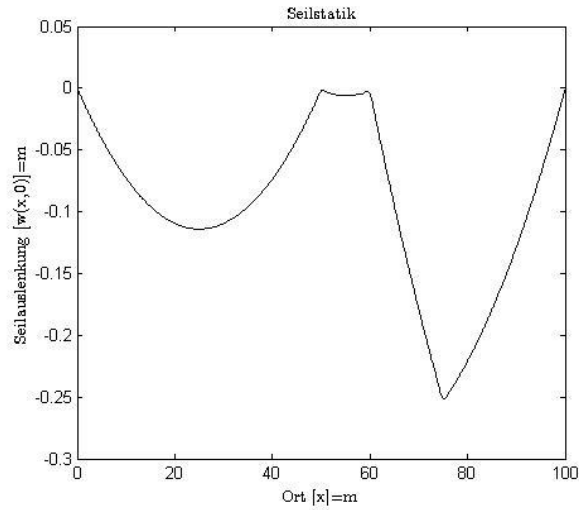
The maximum deflection in this case is -0.35.

The mass of the cabin has a direct influence of the deflection of the rope and if the system parameters is changed, the deflection also will be changed. For example if the m_f is 800 instead of 400.



The maximum deflection according to heavier mass will be -0.6m.

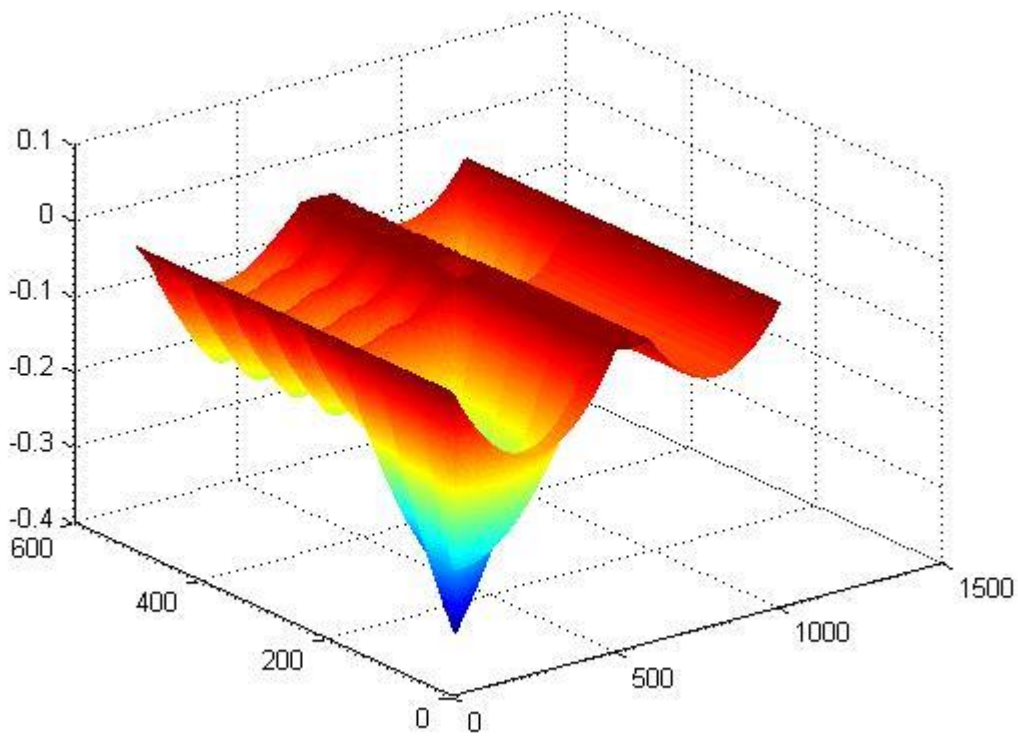
The initial condition where the m_f is hanging can also vary but not influence the deflection of the rope if the distribution is symmetric and the sheaves are positioned at the middle. Here the results with $m_f = 400kg$ but the cabin is hanging at 75m. The position of the sheaves are the same.



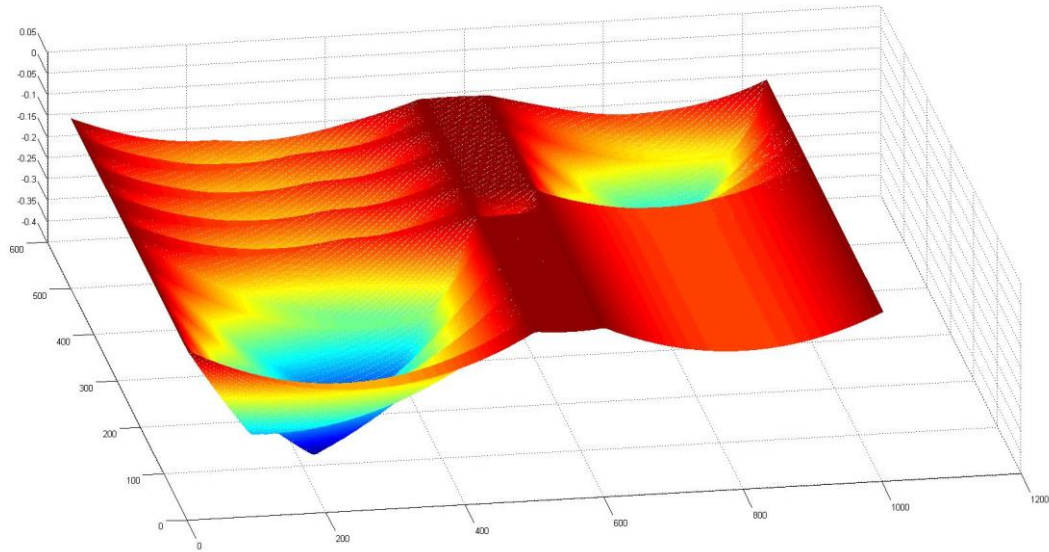
The deflection is lower because the sheaves are not exactly at $\frac{L}{2} \pm x$.

2.4.1.2 Dynamic Simulation Results and discuss

Dynamic results of the first level and interpretation of the diagrams



In dynamic area we can see the first sheave at 50m and the second one at 60m. The both sheaves are permanently fixed to their position and can't move. The cabin is 400Kg with the velocity of 20m/s needs 5 sec to pass the 100m rope field from the starting point.



The hollow area at the between 2.5 and 3 second shows transient area at the time that cabin is transferred from left to right side and at this time is exactly between two sheaves and causes the deflection in this period of time.

2.4.2 Modeling the second level with vertically free sheaves

In the second layer, each sheave is assembled on virtual spring so that it can swing on the vertical position. The mass of the sheaves is considered in this level as $m_{R1} = m_{R2} = m_R$.

$\mu \cdot \ddot{w} - s \cdot w'' = \overbrace{-\mu \cdot g}^{\text{Gravity}} - \overbrace{F_{R1} \cdot f_1(x)}^{\text{First sheave}} - \overbrace{F_{R2} \cdot f_2(x)}^{\text{Second sheave}} - \overbrace{F_f \cdot f_f(x)}^{\text{Cabin}}$	Characteristic equation of the rope
$m_{R1} \cdot \ddot{y}_{R1} = -m_{R1} \cdot g + F_{F1} - F_{R1}$	Characteristic equation of the first sheave
$m_{R2} \cdot \ddot{y}_{R2} = -m_{R2} \cdot g + F_{F2} - F_{R2}$	Characteristic equation of the second sheave
$m_f \cdot \ddot{y} = -m_f \cdot g + F_f$	Characteristic equation of the Cabin

Calculating the reaction forces of the sheaves hanging on the springs:

$$F_{R1} = -k_R \left(\begin{matrix} \text{Set point} \\ \widehat{y}_{R1} \end{matrix} - w(x_{R1}, t) \right) = -k_R (y_{R1} - \vec{C}^T(x_{R1}) \cdot T)$$

$$F_{R2} = -k_R \left(\begin{matrix} \text{Set point} \\ \widehat{y}_{R2} \end{matrix} - w(x_{R2}, t) \right) = -k_R (y_{R2} - \vec{C}^T(x_{R2}) \cdot T)$$

$$F_{F1} = -c(L_0 - y_{R1})$$

$$F_{F2} = -c(L_0 - y_{R2})$$

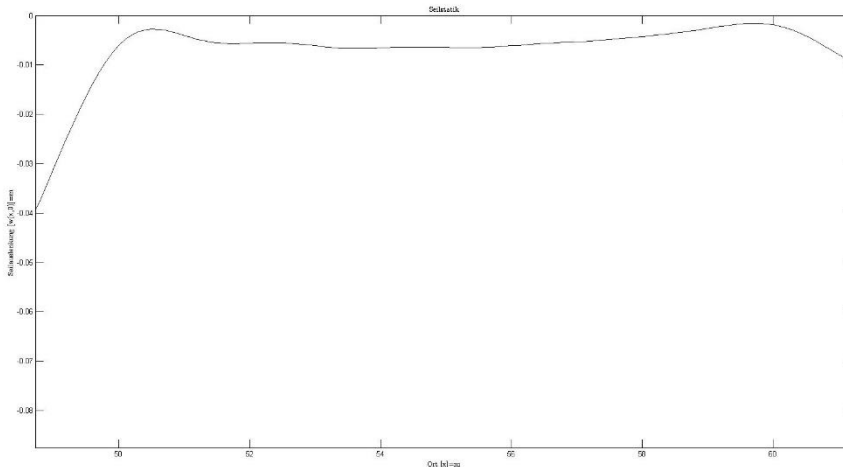
$$F_f = -k_R \left(\begin{matrix} \text{Set point} \\ \widehat{y}_f \end{matrix} - w(x_p, t) \right) = -k_R (y_f - \vec{C}^T(x_p) \cdot T)$$

Using Galerkin method in this level will result:

$$M \cdot \ddot{T} + K \cdot T = +E_g - F_{R1} \cdot E_{R1} - F_{R2} \cdot E_{R2} - F_f \cdot E(t)$$

$$M \cdot \ddot{T} + K \cdot T = +\mu \cdot g + F_{R1} \cdot \delta(x - x_{R1}) + F_{R2} \cdot \delta(x - x_{R2}) - F_f \cdot \delta \left(x - \overbrace{x_p}^{\frac{v \cdot t}{L}} \right)$$

2.4.2.1 Static Simulation Results and discuss

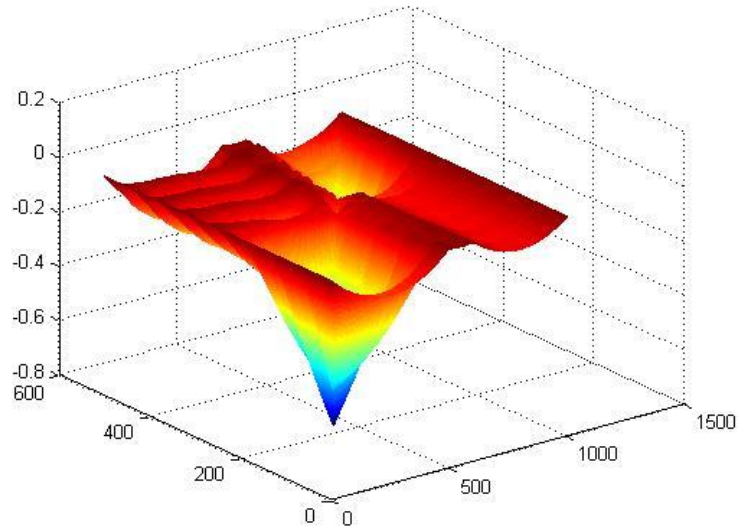


As seen the first sheave reacts to the heavier side of the rope and due to bigger reaction force pushes the sheaves down. The second sheave has to bear a lighter weight and approximately stay at the same position.

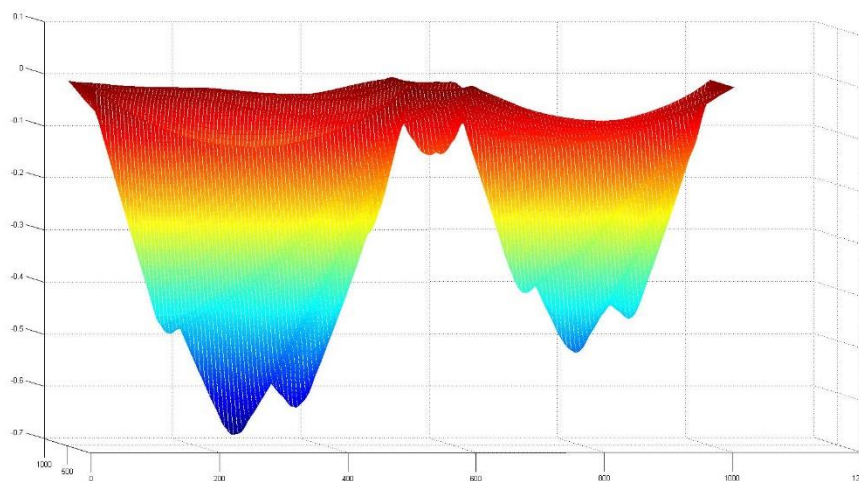
Results of the second level (pressure through the forces on the springs) $m_f=800$ $v=20$ t_5

2.4.2.2 Dynamic Simulation Results and discuss

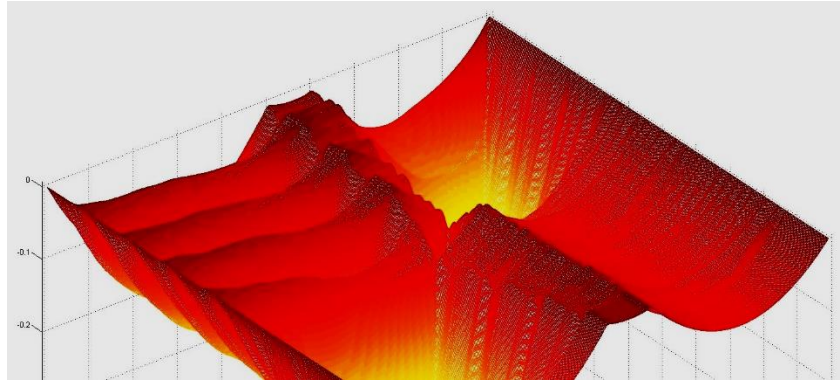
Dynamic results are made with the mass of $m_f=800$, velocity of 20 m/s and simulation time of 5sec. Also here the cabin starts from beginning of 100m rope and passes the whole route in 5sec.



The main difference to the first level is the reaction of the sheaves (which can move vertically in the second level) due to different pressure which comes from the reaction forces.



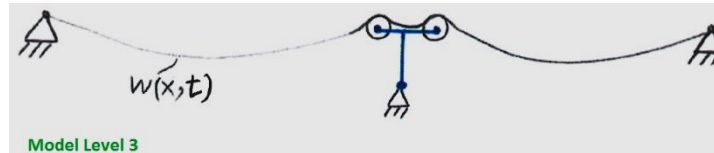
The picture above shows a better view the deflection of the rope at the time that cabin passes over the sheaves (in the middle). For better understanding of this phenomenon the sheaves are defined with a distance of 10m so that the middle area can be studied closely.



In the picture above the reactions of the sheaves to the heavier side of the rope is demonstrated. Heavier left side (if the cabin is on the left side) pushes the first sheave down until the cabin is transferred to the right. The time between when the cabin is at the middle of the sheaves pushes the both sheaves in $-x$ direction. And finally when the cabin passes to the right side, the reaction force on the second sheaves pushes it down and the first sheave comes up.

2.4.3 Modeling the third level with vertically and rotationally free sheaves

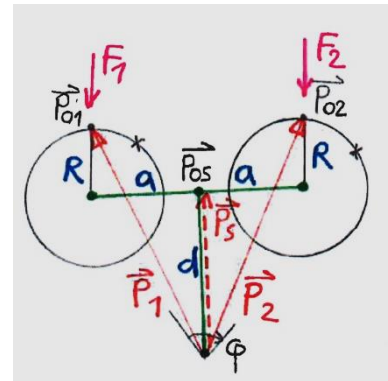
In the third layer the sheaves are connected to each other and dependent on the mass of the cabin and position of the sheaves assembly they can move in horizontal and respectively in vertical direction. In this level the model is completely simulated and in compare of the last two simulations level 1 and level 2 are a restricted and special cases of the third level.



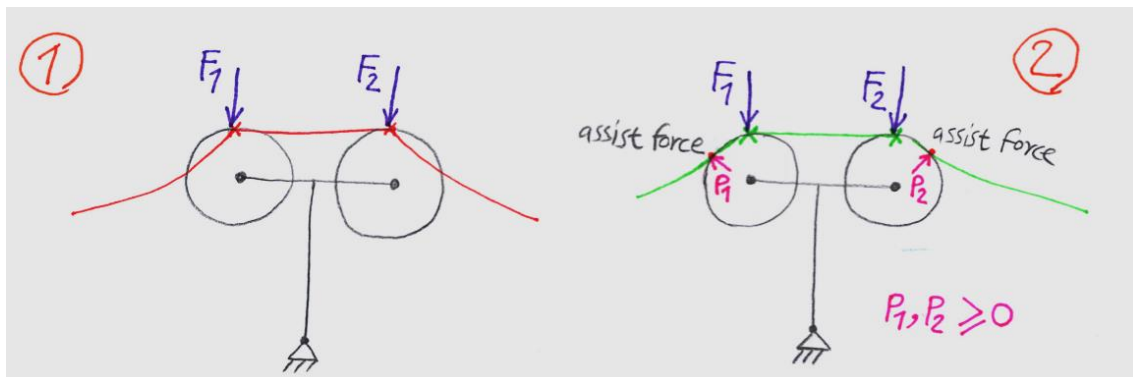
2.4.3.1 Defining Generalized Coordinates

To define the kinematics of the sheaves assembly in this case, a generalized coordination is used to simplify and demonstrate the movement-rotation of the sheaves assembly which depends on angle φ in the both directions.

The reaction forces F_1 and F_2 are not affecting the sheaves vertically as demonstrated, theoretically they will act angular on the sheaves but because of the ration of the sheave diameters (very small) to the rope field (very long) this forces are approximated vertically on the contact points P_{o1} and P_{o2} on the sheaves. This simplification will not influence the end results of the calculations.



The problem that here occurs because of the vertically affecting reaction forces is that in this case the rope can physically stick inside the sheave. To avoid this, mathematical inequalities are used to define a reaction force at the outer edge of the sheave that doesn't let the rope to stick inside the sheave. This force has to be positive permanently and a negative value means that the rope is already inside the sheave that should not happen. –this method is implemented in software simulation with Matlab. The pictures below demonstrate this physical phenomenon and how to handle it mathematical and mechanically.



2.4.3.2 Kinematics and Rotation

To define the kinematics of the systems in third level the position of the sheaves assembly is defined in a generalized coordinate. This position depends on the angle of ϕ .

The rotation matrix *Rot* will demonstrate the displacement of the sheaves assembly in different directions depending the mass of the cabin m_f and the position of the sheaves and the weight of the rope field in each side of the sheaves assembly.

$$P_{01} = \begin{bmatrix} -a \\ d+R \end{bmatrix}, P_{02} = \begin{bmatrix} a \\ d+R \end{bmatrix}, P_{0s} = \begin{bmatrix} 0 \\ d \end{bmatrix}$$

$$Rot = \begin{bmatrix} \cos\phi & -\sin\phi \\ \sin\phi & \cos\phi \end{bmatrix}, l_x = \begin{bmatrix} 1 \\ 0 \end{bmatrix}, l_y = \begin{bmatrix} 0 \\ 1 \end{bmatrix}$$

$$\vec{P}_1(t) = \vec{P}_{01} \cdot Rot, P_2(t) = \vec{P}_{02} \cdot Rot, \vec{P}_s(t) = \vec{P}_{0s} \cdot Rot \quad \begin{cases} x_1 = \vec{P}_1 \cdot l_x \\ x_2 = P_2 \cdot l_x \end{cases}$$

Using the weighted residuum method of Galerkin will result:

$$\mu \ddot{w} - (S\dot{w})' = -\mu g - F_1 \delta(x-x_1) - F_2 \delta(x-x_2)$$

$$L(x) = \mu \ddot{w} - (S\dot{w})' + \mu g + F_1 \delta(x-x_1) + F_2 \delta(x-x_2) \quad \text{Galerkin}$$

$$\int_0^L e(x) y(x) dx = 0, y(x) = \vec{c}(x)$$

$$M\ddot{T} + KT = E_g - F_1 E_1 - F_2 E_2$$

$$F_1(t) = -K_R (\vec{P}_1 \cdot \vec{l}_y - \vec{c}^T(x_1) \cdot T), \vec{c}^T(x_1) = [\sin \frac{\pi}{L} (\vec{P}_1 \cdot \vec{l}_x) \dots \sin \frac{n\pi}{L} (\vec{P}_1 \cdot \vec{l}_x)]$$

$$F_2(t) = -K_R (\vec{P}_2 \cdot \vec{l}_y - \vec{c}^T(x_2) \cdot T), \vec{c}^T(x_2) = [\sin \frac{\pi}{L} (\vec{P}_2 \cdot \vec{l}_x) \dots \sin \frac{n\pi}{L} (\vec{P}_2 \cdot \vec{l}_x)]$$

We developed unique finite elements carrying a moving mass particle. It was not yet the general solution for practitioners. In engineering practice real structures possess a characteristic critical speed (of the load) in a range of about 200 km/h (in the case of railway tracks) and this can vary depending on structural details and environmental conditions.

2.4.3.3 Steady States formulation

Static.

$$M\ddot{T}=0 \rightarrow KT_0 = E_g - F_1 \cdot E_1 - F_2 \cdot E_2$$

$$KT_0 = E_g + K_R (\vec{P}_1 \cdot \vec{l}_y - \vec{C}^T(x_1) \cdot T_0) E_1 + K_R (\vec{P}_2 \cdot \vec{l}_y - \vec{C}^T(x_2) \cdot T_0) E_2$$

$$KT_0 = E_g + K_R E_1 \vec{P}_1 \vec{l}_y - K_R E_1 \vec{C}^T(x_1) T_0 + K_R E_2 \vec{P}_2 \vec{l}_y - K_R E_2 \vec{C}^T(x_2) T_0$$

$$(K + K_R E_1 \vec{C}^T(x_1) + K_R E_2 \vec{C}^T(x_2)) T_0 = E_g + K_R E_1 \vec{P}_1 \vec{l}_y + K_R E_2 \vec{P}_2 \vec{l}_y$$

K_{ges}

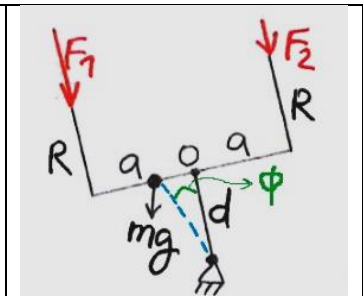
$$T_0 = K_{ges}^{-1} (E_g + K_R E_1 \vec{P}_1 \vec{l}_y + K_R E_2 \vec{P}_2 \vec{l}_y)$$

$$E_1 = \int_0^L \delta(x-x_1) \vec{C}(x) dx = \vec{C}(x_1)$$

$$E_2 = \int_0^L \delta(x-x_2) \vec{C}(x) dx = \vec{C}(x_2)$$

2.4.3.4 Optimizing and balancing the Momentum

The sheaves assembly has to react correctly to the right and left side depending on the rope and the mass of the cabin in static and dynamic mode. To make this possible the static idle mode should be calculated, regarding the reaction forces F_1 and F_2 . The momentum resulting from the difference of reaction forces in the middle of the sheaves assembly should be balanced through the angle of ϕ . This balance will be defined in the following way:



$$\sum M = 0$$

$$M_0 = F_1 \vec{P}_1 \vec{l}_x + mg \vec{P}_s \vec{l}_x - F_2 \vec{P}_2 \vec{l}_x$$

As seen due to the rotation of the sheaves mechanism depending on ϕ , the center of the gravity is also shifted depending on the vector of \vec{P}_s .

To start the optimization process, a first value of ϕ and the distances of a , R and d are needed to calculate the *Rot* or the value of rotation matrix. After that the vectors of \vec{P}_1 , \vec{P}_2 and \vec{P}_s are calculated. This values are needed to calculate the T_0 and finally the momentum will result from this values and the reaction forces of $F_1(t)$ and $F_2(t)$. This will continue in form of an interpolation process to find the correct value of ϕ that balances the system and makes the momentum equal to zero.

$\phi \rightarrow Rot$ **in circle form**
 $a, R, d, Rot \rightarrow \vec{P}_1, \vec{P}_2, \vec{P}_S \rightarrow T_0 \rightarrow F_1(t), F_2(t) \rightarrow M_0 \neq 0 \text{ (}\phi\text{)}$

2.4.3.5 Kinetics

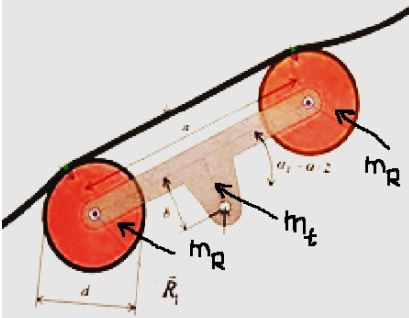
In compare of level one and two, and because of the generalized coordinate to define the movement of the sheaves assembly, a second equation is applied to the system to fulfill the kinematic requirements of the system. This equation is ϕ dependent and indirectly define the momentum which comes as a result of the reaction forces on the rope.

$$\begin{cases} M\ddot{T} + KT = -Eg - F_1 \delta(x-x_1) - F_2 \delta(x-x_2) \\ J\ddot{\phi} = mg \vec{P}_S \vec{l}_x + F_1 \vec{P}_1 \vec{l}_x - F_2 \vec{P}_2 \vec{l}_x \end{cases}$$

The moment of inertia which is multiplied with the second time derivation of the ϕ comes from:

$$J_z = \sum_i m_i (x_i^2 + y_i^2)$$

Which m_i in this case consists of the mass of the both sheaves m_R (which are the same) and mass of the body of the sheaves mechanism m_0 . This has to multiplied with the real part of the vector \vec{P}_S so that:

$J = J_0 + (m_0 + 2m_R) (\vec{P}_S ^2)$	
--	--

The simplification of both equations for T and ϕ will result:

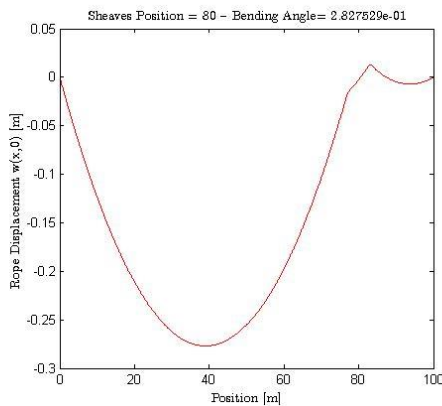
$$\ddot{T} = -M^{-1}KT - M^{-1}Eg - M^{-1}F_1\delta(x-x_1) - M^{-1}F_2\delta(x-x_2)$$

$$\ddot{\phi} = J^{-1}mg\vec{P}_S\vec{l}_x + J^{-1}F_1\vec{P}_1\vec{l}_x - J^{-1}F_2\vec{P}_2\vec{l}_x$$

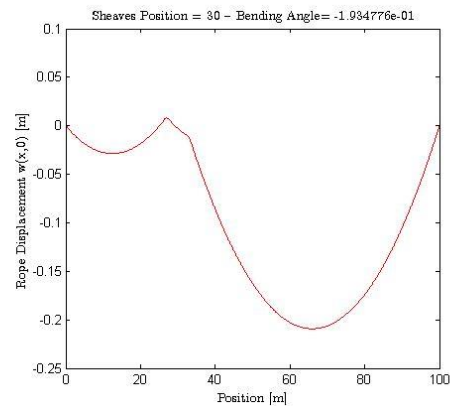
$$X = \begin{bmatrix} T \\ \phi \\ \dot{T} \\ \dot{\phi} \end{bmatrix}$$

2.4.3.6 Static results and discuss

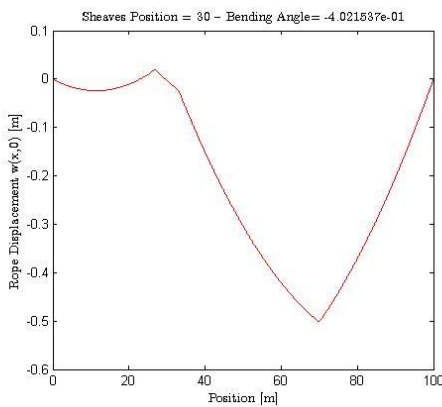
If the system simulated without the cabin and the position of the sheaves assembly is at the middle of the rope field, the angle of ϕ will be zero because the systems is symmetric. If we push the sheaves assembly to the right or left side (no cabin is considered) the weight of the rope field will be heavier in one side than the other. So the sheaves assembly will bend to the side which is heavier. In this case the angle of ϕ is defined positive value if the sheaves assembly is bended to the left side.



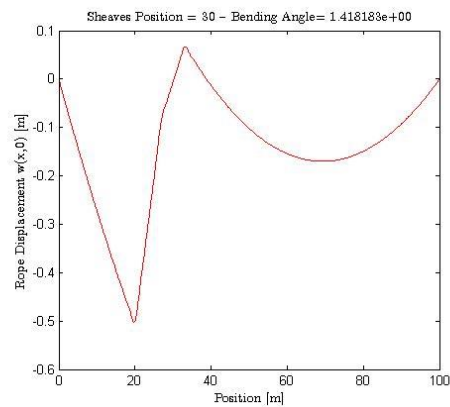
Without mass and sheaves assembly in right



Without mass and sheaves assembly in left



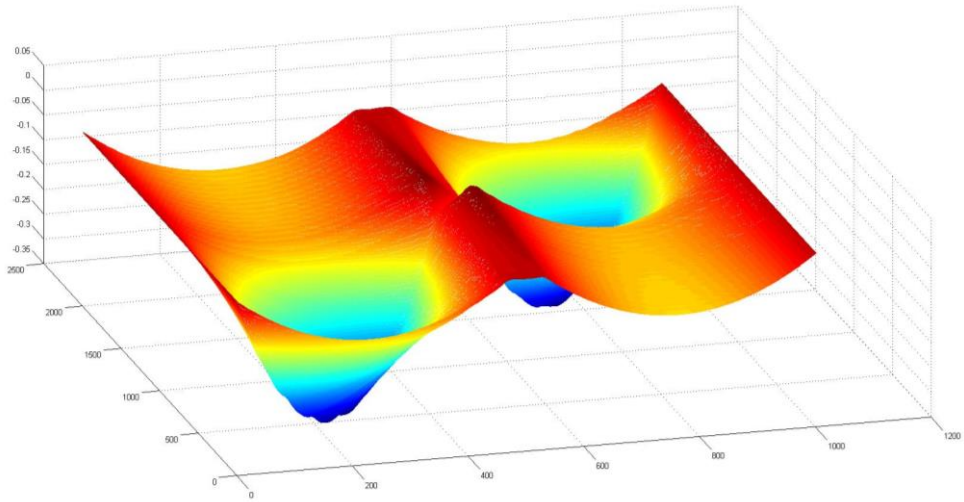
With mass at right and sheaves assembly in left



With mass at left and sheaves assembly in left

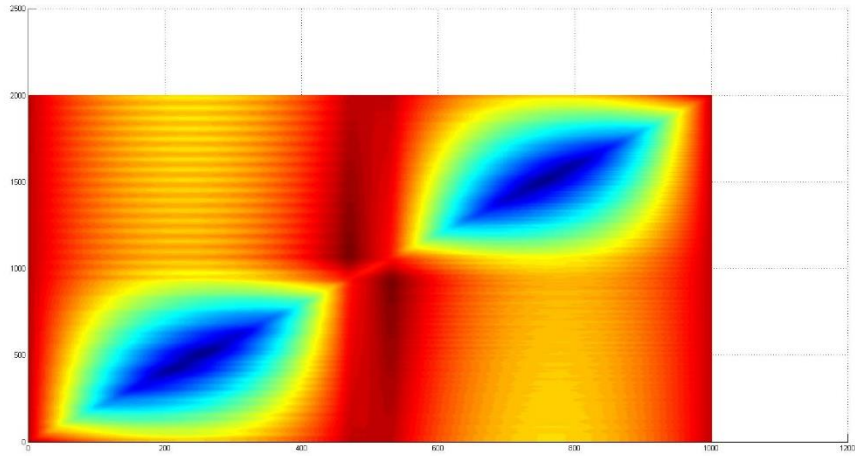
2.4.3.7 Dynamic Results and discuss

Dynamic results of the third level and interpretation of the diagrams.



As seen the mechanism of the connected sheaves assembly in the this level reacts to the passing vehicle by correcting its angle in the direction which more loads comes from. This simulation is made with 5 m/s, a rope length of 100 m and velocity of 20 m/s.

Considering the route of the vehicle from time and displacement axis will show this results.



As expected the maximum deflection occurs in the middle of the each rope filed, which here is marked as dark blue. Up to now all the simulations are made with a constant rope tension.

2.5 Contact Mechanics

The goal in this chapter will be to relate the sheave to the rope by means of a virtual spring which has a very high stiffness. This will be the simplest method to define the contact as a point and not as a surface.

Here we will have a dirac impulse which is used to define the contact between sheave /sheaves assembly and the rope is a good approximation for the contact mechanics.

It has to be considered that a very high spring stiffness can lead to high frequency vibration in the results that can influence specially the dynamical results of the system in this level. The stiffness that is used in this level is 10^6 and because of that there are backlashes in the sheave assembly when the cabin is moving through the support to the second field of the system. Even optimizing the system or taking small steps for the ODE solver cannot eliminate the small high frequency vibration.

There are two different types of ODE solvers are used in the matlab code to have a comparison between the solutions. ODE15S and ODE45. The documented results are made with ODE45 because the simulation is more efficient and time steps don't influence the results as it is in ODE15S.

The other problem with the contact mechanic is that because the system is mathematically by means of partial differential equation simulated and not with multibody basis, it is possible that the rope can go through the sheave at the point that it is coming from the field one to the center of the system. This phenomenon can have avoided by using the Boolean logic that filters the intersection of the system which is used generally and shared between the sheave and the rope.

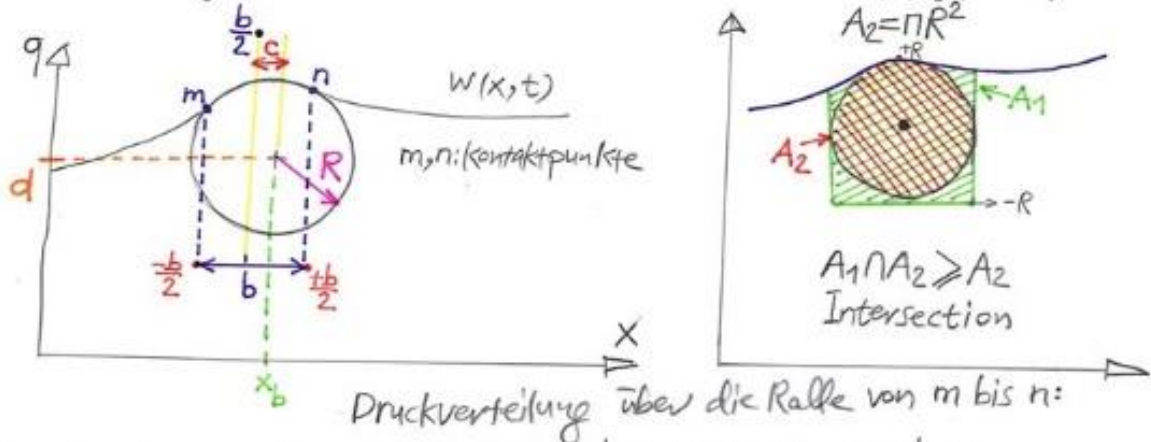
Admittedly, this cannot happen in this case because of the scale of the system. In other words, the scale of the sheaves that are used here proportionally is much smaller than the rope fields in both sides. Because of that when the rope comes from both fields to the center of the system there is just a very small surface that makes the contact between rope and sheave.

In the calculation below is defined how the intersection point should be mathematically defined to avoid the general intersection.

$$\Pi = \frac{1}{2} \int_0^L [E_{kin} - E_{pot}] dx$$

(Hamiltonische Formulierung)
Energiefunktional des Seils

$$\Pi_{stat} = \frac{1}{2} \int_0^L [S \dot{w}(x)^2 - 2W(x)(-Mg + q(x))] dx$$



$$q(x) = (-a(x - x_b - c)^2 + d) (\sigma(x - x_b - c - \frac{b}{2}) - \sigma(x - x_b - c + \frac{b}{2}))$$

$$Ritz: W(x,t) = \sum_{n=1}^N p_k \sin(\frac{n\pi}{L}x) = C^T P$$

$$q_T(x) = q_0 + q(x), \quad q_T(x) = \sum_{n=1}^N q_k \sin(\frac{n\pi}{L}x) = C^T q \quad \text{seil}$$

$$\Pi = \frac{1}{2} \int_0^L [S(C^T P)^2 - 2(C^T q)(C^T P)] dx$$

$$\int_{x_b - c - \frac{b}{2}}^{x_b - c + \frac{b}{2}} W(x) dx \geq \int_{x_b - c - \frac{b}{2}}^{x_b - c + \frac{b}{2}} W(x)_{Ralle} dx$$

Seil darf nicht in die Ralle stecken.
 $y(x) \geq y_{Ralle} \rightarrow g_T = y_{Ralle} - C^T P \leq 0$

$$\mathcal{L}(a, b, c, d, x) = \min \quad \text{KKT-Optimierung}$$

The advantages of the analytical method allowed us to exhibit an interesting feature of the solution of the differential equation governing the motion of the string near an end support. It is visible in Figures above. The diagrams exhibit jumps of the mass displacement in time. Let us consider the physical nature of these jumps. The simplest explanation can be based on the force equilibrium. We must remember that a constant string tension N is the fundamental assumption in our problem. Moreover, in Figure 2.3 the horizontal force pushing the mass to hold the speed v must be seen in the scheme. At the final stage (as depicted in Figure), the remaining distance d

will be traversed in time d/v . In this period, the mass m must be lifted from the position w_B to zero. If the deflection w_B is high enough, compared to the other parameters, the necessary acceleration applied to the mass must result in high forces on the string F . In such a case, F can exceed N if m or v is sufficiently high. This fact violates our assumptions and the condition of applicability of the small vibration equation $(\partial w/\partial x)^2 \ll 1$.

A mathematical proof can be given only in the particular case. In the general case, only numerical simulations can be carried out. But this part of the research is still not finished and needs more calculations.

3 Limits of the semi-analytical solution on moving load

This chapter is about the numerical approaches to the moving load problem given in the literature. Most of them concern beam deflection. Unfortunately, comparison with exact analytical or semi-analytical results are rarely given. In most cases the authors compare their results with curves published by other researchers.

The authors compute examples using different data and boundary conditions. They usually emphasize the agreement of their results with other computational methods. Unfortunately, results which coincide with an approximate method are not necessarily accurate as well. We should relate the results to analytical solutions or at least to solutions which fulfill the governing differential equations with possibly the lowest error. In this chapter we will compare the curves presented in these publications with semi-analytical results.

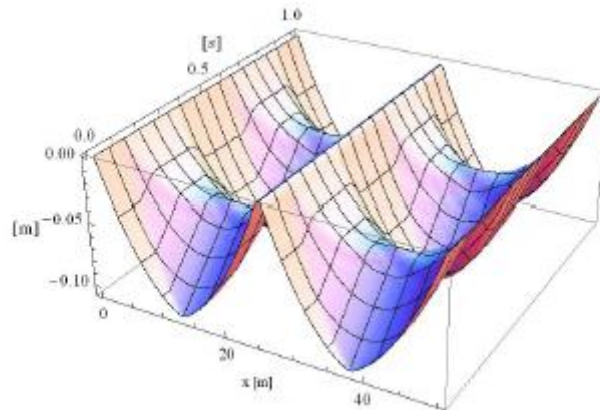
First we will consider a string, although this type of a structure is not frequently studied in the literature. Then we will describe the Bernoulli–Euler beam and the Timoshenko beam. The approaches in the literature deal with a moving non-inertial force and an inertial force. Some of them are devoted to a system with a point load or a distributed load.

Some published papers, even ones extensively cited by other authors, do not give an objective measure of the error. The authors claim that a slight visual coincidence with other curves proves its correctness. Moreover, they expect that differences in the results justify the advantages of the published approach and should convince one of its correctness.

First of all, we must warn against using an inertial mass on nodes of the mesh. The mass distribution proportional to the distances to the nodal points fails, and the results can not be accepted. In the case of a beam we are dealing with a parabolic differential equation in space. This fact results in smooth and infinitely fast bending of the entire structure. The local deformation is strongly influenced by other parts of the beam. The influence of a concentrated load of a different type is lower than in the case of a string or a membrane.

The development of computer methods has led to a series of works on numerical calculations, especially using the finite element method (FEM). This method is much more comprehensive than the analytical or semi-analytical methods. Papers

discussing moving loads with constant or periodic amplitude are simple and rely on modifying the vector on the right hand side, step by step. The resulting work is presented in papers devoted to modelling the motion of a vehicle as a group of oscillators. These problems require the coincidence of the displacements and forces of two subsystems: the main structure and the moving oscillator as shown in the results below.



For balancing the respective quantities in both systems a simple iterative procedure is applied. This method also involves a modification of the right-hand side vector. At the first stage the structure is loaded by dynamic forces at the contact points corresponding with the oscillators. As a result, the nodal displacements of a discrete structure are obtained. This allows us to determine the vertical displacement of a beam or a plate at the contact points with the oscillators. Displacements assumed as boundary conditions force the motion of the oscillator. This iterative procedure results in force–displacement equilibrium in a single time step. Unfortunately, the convergence of such a scheme is limited to a certain range of parameters, such as the travelling velocity, stiffness of the structure, inertia, and especially the time step. Otherwise the iterative procedure must be more complex and time consuming.

The insertion of the inertia of the moving load effect requires not only a modification of the right-hand side vector, but also selected parts of the global inertia, damping, and stiffness matrices of the system, in every time step. The first study discussing the influence of the inertia of the moving mass was reported in.

An inertial load moving at a constant speed on the Euler beam was considered. Further works are also related to beams or plates in which the nodal displacements and angles are interpolated by cubic polynomials. In these papers the derived matrices are not general. They are not suitable for use for the string or Timoshenko beam in which the nodal displacements and angles are interpolated by a linear function independently. In the literature, you can also find examples of the discrete element method for moving loads. This consists of replacing a beam by a system of rigid rods, connected among themselves on the basis of the compatibility of the rotation of adjacent elements. The acceleration of a mass particle in the space-time domain is described by the Renaud formula. The different parts of the equation describe the lateral acceleration, Coriolis acceleration and centrifugal acceleration. The interpolation of the nodal displacements by a third order polynomial allows us to derive the matrices responsible

for the travelling mass particle. Unfortunately, the Euler beam equation is not a wave equation. The study of a wave phenomenon is possible by using a more complex model of the Timoshenko beam in which the vibration equation takes into account the influence of lateral forces and rotatory inertia on the deflection line of the beam. The angle formed by the axis of the deformed beam is composed of the pure bending angle and the angle corresponding to the deformation of the pure shear. Independent interpolation of displacements and rotation angles of the Timoshenko beam causes serious problems. Linear interpolation of nodal shape features renders impossible the designation of the centrifugal acceleration of a moving mass particle. In the previous works, we presented a method for determining the matrices responsible for the description of the moving mass by the space-time finite Oscillator element method with the use of a linear interpolation.

4 Conclusion

The semi analytical methods which are used here, combining Galerkin method and numerical calculation of Runge Kutta 4th and 5th order are used at Massachusetts Institute of Technology for considering the dynamical stability of nondeterministic and also chaotic systems.

But the method that I used in my PhD thesis is a new combination of this two methods. Normally for analysing the complex systems in continuum mechanics one of the methods above applied to study the systems. The problem is if a dynamical system is not discrete, the methods that are available are either the analytical methods which need a huge amount of calculations and are very time consuming, or the numerical methods which are faster than analytical methods but not precise and accrue enough and sometimes the results are not reliable. But combining these two methods inside a multi paradigm numerical software can optimize the analysis and give an accuracy above 98% and is extremely faster than the analytical methods.

The goal of this research was to develop a new hybrid method to observe and analyze the chaotic dynamical systems and find a new way to optimize the numerical/analytical solutions for the nondeterministic system. This research stay in the Harvard/MIT science and technology division helped me to achieve this goal and optimize my dissertation which I am going to submit this year (2018-2019).

At the end I would like to thank Marshall plan foundation for making this scientific cooperation between these two universities possible.